AMERICAN SOCIETY FOR MICROBIOLOGY | Journal of Virology®

VIRUS-CELL INTERACTIONS

CD300lf Conditional Knockout Mouse Reveals Strain-Specific Cellular Tropism of Murine Norovirus

Vincent R. Graziano,[a,b] Mia Madel Alfajaro,[a,b] Cameron O. Schmitz,[a,b] Renata B. Filler,[a,b] Madison S. Strine,[a,b] Jin Wei,[a,b] Leon L. Hsieh,[c] Megan T. Baldridge,[d] Timothy J. Nice,[e] Sanghyun Lee,[f] Robert C. Orchard,[g] Craig B. Wilen[a,b]

[a]Department of Laboratory Medicine, Yale University School of Medicine, New Haven, Connecticut, USA
[b]Department of Immunobiology, Yale University School of Medicine, New Haven, Connecticut, USA
[c]Department of Molecular Microbiology and Immunology, Bloomberg School of Public Health, Johns Hopkins University, Baltimore, Maryland, USA
[d]Department of Medicine, Division of Infectious Diseases, Edison Family Center for Genome Sciences & Systems Biology, Washington University School of Medicine, Saint Louis, Missouri, USA
[e]Department of Molecular Microbiology and Immunology, Oregon Health and Science University, Portland, Oregon, USA
[f]Department of Molecular Microbiology and Immunology, Brown University, Providence, Rhode Island, USA
[g]Department of Immunology, University of Texas Southwestern Medical School, Dallas, Texas, USA

ABSTRACT Noroviruses are a leading cause of gastrointestinal infection in humans and mice. Understanding human norovirus (HuNoV) cell tropism has important implications for our understanding of viral pathogenesis. Murine norovirus (MNoV) is extensively used as a surrogate model for HuNoV. We previously identified CD300lf as the receptor for MNoV. Here, we generated a *Cd300lf* conditional knockout (*CD300lf*$^{F/F}$) mouse to elucidate the cell tropism of persistent and nonpersistent strains of murine norovirus. Using this mouse model, we demonstrated that CD300lf expression on intestinal epithelial cells (IECs), and on tuft cells in particular, is essential for transmission of the persistent MNoV strain CR6 (MNoV^{CR6}) *in vivo*. In contrast, the nonpersistent MNoV strain CW3 (MNoV^{CW3}) does not require CD300lf expression on IECs for infection. However, deletion of CD300lf in myelomonocytic cells (*LysM Cre*+) partially reduces CW3 viral load in lymphoid and intestinal tissues. Disruption of CD300lf expression on B cells (*CD19 Cre*), neutrophils (*Mrp8 Cre*), and dendritic cells (*CD11c Cre*) did not affect MNoV^{CW3} viral RNA levels. Finally, we show that the transcription factor STAT1, which is critical for the innate immune response, partially restricts the cell tropism of MNoV^{CW3} to LysM+ cells. Taken together, these data demonstrate that CD300lf expression on tuft cells is essential for MNoV^{CR6}; that myelomonocytic cells are a major, but not exclusive, target cell of MNoV^{CW3}; and that STAT1 signaling restricts the cellular tropism of MNoV^{CW3}. This study provides the first genetic system for studying the cell type-specific role of CD300lf in norovirus pathogenesis.

IMPORTANCE Human noroviruses (HuNoVs) are a leading cause of gastroenteritis resulting in up to 200,000 deaths each year. The receptor and cell tropism of HuNoV in immunocompetent humans are unclear. We use murine norovirus (MNoV) as a model for HuNoV. We recently identified CD300lf as the sole physiologic receptor for MNoV. Here, we leverage this finding to generate a *Cd300lf* conditional knockout mouse to decipher the contributions of specific cell types to MNoV infection. We demonstrate that persistent MNoV^{CR6} requires CD300lf expression on tuft cells. In contrast, multiple CD300lf+ cell types, dominated by myelomonocytic cells, are sufficient for nonpersistent MNoV^{CW3} infection. CD300lf expression on epithelial cells, B cells, neutrophils, and dendritic cells is not critical for MNoV^{CW3} infection. Mortality associated with the MNoV^{CW3} strain in *Stat1*$^{-/-}$ mice does not require CD300lf expression on LysM+ cells, highlighting that both CD300lf receptor expression and innate immunity regulate MNoV cell tropism *in vivo*.

KEYWORDS CD300lf, cell tropism, norovirus, viral entry

Citation Graziano VR, Alfajaro MM, Schmitz CO, Filler RB, Strine MS, Wei J, Hsieh LL, Baldridge MT, Nice TJ, Lee S, Orchard RC, Wilen CB. 2021. CD300lf conditional knockout mouse reveals strain-specific cellular tropism of murine norovirus. J Virol 95:e01652-20. https://doi.org/10.1128/JVI.01652-20.

Editor Rebecca Ellis Dutch, University of Kentucky College of Medicine

Address correspondence to Craig B. Wilen, craig.wilen@yale.edu.

Received 19 August 2020
Accepted 2 November 2020
Accepted manuscript posted online 11 November 2020
Published 13 January 2021

Human noroviruses (HuNoVs) represent a leading cause of gastroenteritis and an important cause of childhood mortality worldwide (1, 2). *Norovirus*, a genus within the family *Caliciviridae*, include nonenveloped, positive-sense, single-stranded RNA viruses that are transmitted through the fecal-oral route. Noroviruses are segregated into seven genogroups (GI to GVII). Genogroups I, II, and IV contain primarily HuNoVs, while GIII, GV, GVI, and GVII contain bovine NoVs, murine NoVs (MNoV), and feline and canine NoVs (3). A complete understanding of the mechanism underlying the pathogenesis and biology of HuNoV infection is still lacking due to limited HuNoV cell culture systems, heterogeneity among NoV isolates, and a lack of infectious molecular clones (4–8). These knowledge gaps have hindered vaccine and antiviral drug development.

Cell tropism is an important determinant of virus transmission, pathogenesis, and immune evasion. A detailed molecular understanding of the host and viral determinants underlying norovirus cell tropism are critical for vaccine and therapeutic development (6). The cell tropism of noroviruses remains incompletely understood (8–10). HuNoV can replicate in stem cell-derived human intestinal enteroids and human B cell-like cell lines *in vitro* (8, 11, 12). Limited HuNoV replication was also recently reported in HEK293T cells (12). Our understanding of HuNoV tropism *in vivo* is largely dependent on samples taken from immunodeficient humans infected with HuNoV or experimentally infected animal models (9, 13–15). HuNoV infection was identified in dendritic cells and B cells of intravenously infected chimpanzees (13), while intestinal epithelial cells (IECs), macrophages, lymphocytes, and dendritic cells have been identified as HuNoV target cells in pig models (14–17). HuNoV-infected intestinal epithelial cells were observed in immunocompromised humans (18). More recently, HuNoV was shown to infect enteroendocrine cells, a rare secretory epithelial cell population that plays a critical role in the gut-brain axis (9). The determinants of cell tropism, including the viral receptor and the specific role of bile salts and glycans, remain unclear for HuNoV (8, 19, 20).

MNoV represents a model for HuNoV and has enabled the identification of important host and viral factors that can regulate NoV replication and pathogenesis *in vitro* and *in vivo* (4, 21–23). MNoV can be efficiently propagated *in vitro* and productively infects mice, thus providing a tractable *in vivo* system for NoV studies (4, 24). MNoV shares many characteristics with HuNoV, including fecal-oral transmission, capsid structure, intestinal replication, and prolonged shedding after acute infection, reflecting asymptomatic HuNoV infection (4, 24, 25). Infectious molecular clones of MNoV have been described with distinct patterns of pathogenesis. MNoV strain CR6 ($MNoV^{CR6}$) causes persistent enteric infection which can spread systemically but fails to induce lethality in type I interferon (IFN)-deficient mice (25, 26). In contrast, MNoV strain CW3 ($MNoV^{CW3}$), an infectious molecular clone derived from MNV-1, causes nonpersistent systemic infection in immunocompetent mice and lethal infection in mice deficient in type I interferon signaling (23, 26, 27). Also, it was recently demonstrated that MNoV strain MNV-1 can cause dose-dependent and mouse strain-dependent diarrhea in neonatal mice (28).

Although genetically similar, minor genetic variants in these MNoV strains confer distinct *in vivo* phenotypes (25, 26, 29, 30). Viral determinants of infection have been mapped to the viral capsid protein VP1 and the viral nonstructural protein NS1 (25–27, 31). Specific amino acid variants have been identified in VP1 that determine enteric and systemic infection and lethality in mice deficient in type I interferon signaling (26). Variants in NS1 enable $MNoV^{CR6}$ to antagonize type III interferon and establish persistent enteric infection (25, 32). The host determinants of infection include both the MNoV receptor CD300lf and the innate immune system (21, 23, 27, 29, 32). CD300lf is a type I integral membrane protein that binds phospholipids on dead and dying cells and can induce pro- or anti-inflammatory signals depending on the specific context (33). CD300lf is expressed on tuft cells and diverse hematopoietic cells, including macrophages, dendritic cells, neutrophils, and B cells (30, 33). CD300lf has been implicated

in the pathogenesis of multiple sclerosis, inflammatory bowel disease, and depression (34–38).

The cell tropisms of MNoV^{CW3} and MNoV^{CR6} are distinct. Our recent discovery of CD300lf as the receptor for MNoV enabled us to determine that radiation-resistant cells are required for MNoV^{CR6} but not MNoV^{CW3} infection. This finding led us to identify intestinal tuft cells, the only epithelial cell type that expresses CD300lf as a major target cell of MNoV^{CR6} (30). Tuft cells are critical regulators of epithelial response to intestinal helminth infection, as they are the primary producers of interleukin-25 (IL-25) (39–41). However, it remains unknown whether tuft cells are essential for MNoV^{CR6} infection. In contrast, MNoV^{CW3} does not require tuft cells to establish infection (30, 42). MNV-1 or MNoV^{CW3} infection has been reported in dendritic cells, macrophages, monocytes, and B cells *in vivo* (10, 43, 44). In *Stat1*-deficient mice, MNoV^{CW3} has been observed in rare epithelial cells consistent with tuft cells (45). While MNoV^{CW3} does not require tuft cells, we recently showed that CD300lf is essential for infection of diverse MNoV strains, including both MNoV^{CW3} and MNoV^{CR6} *in vivo* (29).

To elucidate the cellular tropism of MNoV *in vivo*, here, we developed a *Cd300lf* conditional knockout (*CD300lf*$^{F/F}$) mouse to specifically delete CD300lf from putative MNoV target cells. We demonstrate that CD300lf expression on tuft cells is essential for MNoV^{CR6} but not MNoV^{CW3} infection and that this tropism depends on the viral NS1 protein. We find that ablation of CD300lf on myelomonocytic (LysM+) cells reduces MNoV^{CW3} infection in immunocompetent mice. We did not observe any reduction in MNoV^{CW3} infection with the depletion of CD300lf in epithelial cells, dendritic cells, neutrophils, or B cells. Interestingly, the antiviral effects of CD300lf disruption on LysM+ cells were not observed in *Stat1*-deficient mice, demonstrating that CD300lf and the innate immune system coordinately regulate MNoV tropism. This suggests CD300lf expression on tuft cells is required for MNoV^{CR6} infection, multiple cell types are sufficient for MNoV^{CW3} infection, and innate immunity regulates MNoV^{CW3} tropism.

RESULTS

CD300lf expression on epithelial cells is required for MNoV^{CR6} but not MNoV^{CW3} infection. To elucidate the cellular tropism of MNoV, we generated a *Cd300lf* conditional knockout mouse via CRISPR/Cas9. We inserted LoxP sites flanking exon 3 of *Cd300lf* (*CD300lf*$^{F/F}$) which encodes amino acids 129 to 158 in the ectodomain of CD300lf (Fig. 1A). We first crossed this mouse to an epithelial cell-specific Cre mouse (*Vil1Cre*) to generate mice with epithelial cells deficient in CD300lf. We validated the efficiency of CD300lf deletion in intestinal epithelial cells by flow cytometry (Fig. 1B). CD300lf+ events were significantly enriched in *CD300lf*$^{F/F}$ *Vil1Cre*− mice compared with *CD300lf*$^{F/F}$ *Vil1Cre*+ littermate control mice (Fig. 1B). We then challenged these mice with 10^6 plaque forming units (PFUs) of MNoV^{CR6} and MNoV^{CW3} perorally (PO); harvested mesenteric lymph node (MLN), spleen, ileum, and colon; and assessed viral genome copies via quantitative real-time PCR (qPCR). At 7 days postinfection (dpi), MNoV^{CR6} genome copies were significantly reduced in the MLN, ileum, and colon of *CD300lf*$^{F/F}$ *Vil1Cre*+ mice compared with *Cre*− controls (Fig. 1C, E, and F). MNoV^{CR6} was not detected in the spleens of either *Cre*− or *Cre*+ mice, consistent with prior studies in wild-type (WT) mice (29–31). MNoV^{CR6} was also undetectable in the feces of *Vil1Cre*+ mice, unlike *Cre*− controls (Fig. 1G). Interestingly, MNoV^{CR6} genomes were detected in the MLN, ileum, colon, and feces in a single *CD300lf*$^{F/F}$ *Vil1Cre*+ mouse (Fig. 1C to F); whether this finding reflects the emergence of a novel viral variant is unclear.

In contrast to MNoV^{CR6}, the MNoV^{CW3} viral genome was detected at similar levels in the MLN and spleen of *CD300lf*$^{F/F}$ *Vil1Cre*+ and *Vil1Cre*− mice (Fig. 1C and D). MNoV^{CW3} viral genomes were also detected at similar levels in the ileum and colon of *CD300lf*$^{F/F}$ *Vil1Cre*− and *Cre*+ mice (Fig. 1E and F). MNoV^{CW3} did not robustly shed in the feces of either *Cre*− or *Cre*+ mice, which is consistent with prior findings (Fig. 1G) (25, 30). Together, these results suggest that productive infection of IECs is not required for MNoV^{CW3} infection. Furthermore, these findings suggest that CD300lf expression on epithelial cells is essential for fecal-oral transmission of MNoV^{CR6} but not MNoV^{CW3} (30).

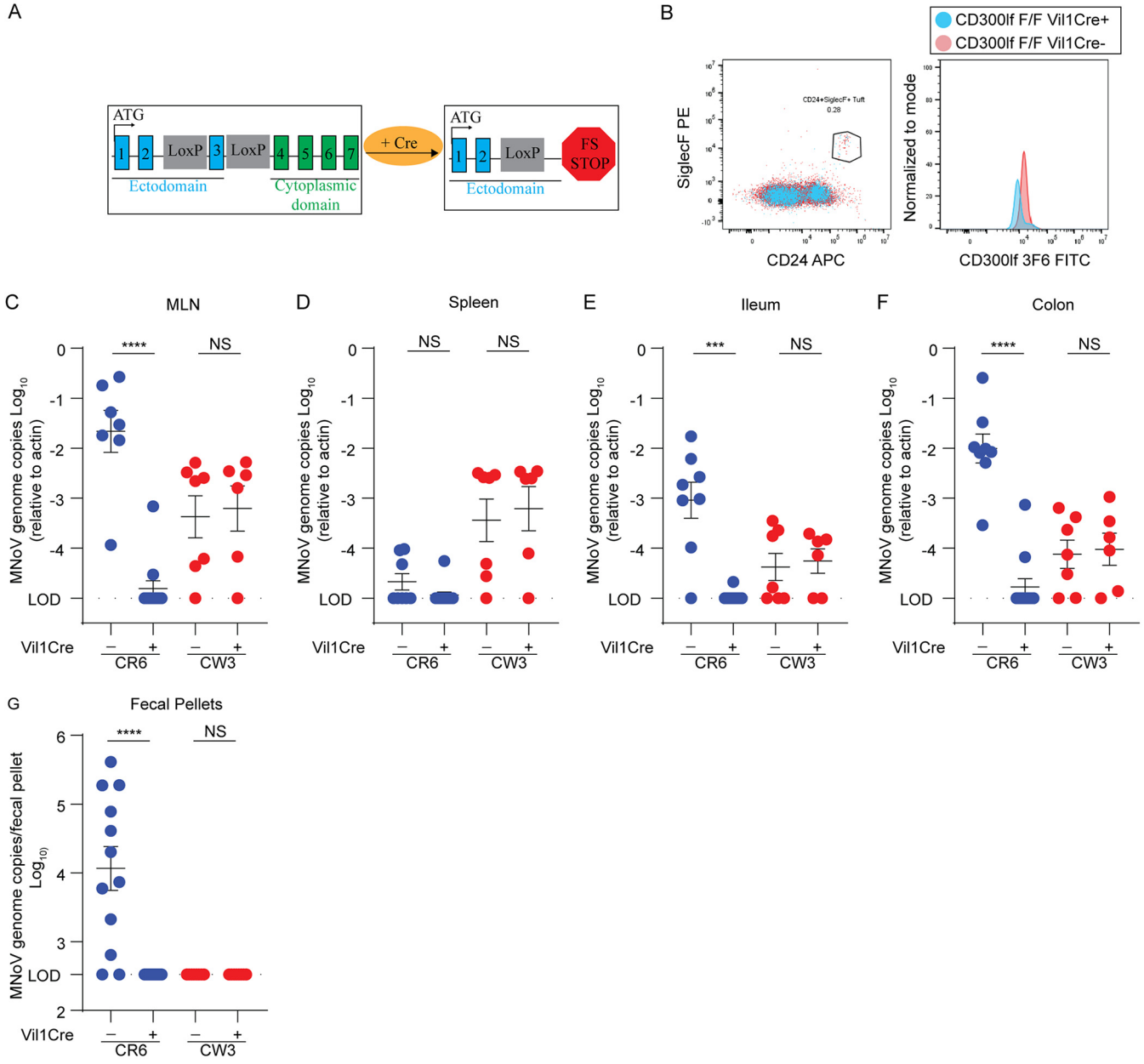

FIG 1 MNoV^{CR6}, but not MNoV^{CW3}, infection requires CD300lf-expressing epithelial cells. (A) Schematic depicting the *Cd300lf* gene locus used to cross with specific cell lineage mouse strains. (B) CD300lf expression is ablated on *Vil1Cre*+ mice as observed via FACS. (C to F) *CD300lf*$^{F/F}$ *Vil1Cre* mice were perorally (PO) infected with 10^6 PFU of MNoV^{CR6} or MNoV^{CW3} and sacrificed at 7 days postinfection (dpi). Tissue titers for MLN (C), spleen (D), ileum (E), or colon (F) were analyzed via qPCR for MNoV genome copies and normalized to actin. Fecal pellets (G) collected at 7 dpi were analyzed via qPCR for MNoV genome copies. Mouse experiments were performed using littermate controls with at least two independent repeats analyzed via Mann-Whitney test. Statistical significance annotated as follows: ****, $P < 0.0001$; ***, $P < 0.001$; NS, not significant.

CD300lf expression on tuft cells is required for MNoV^{CR6} and MNoV$^{CW3\text{-}NS1\text{-}CR6}$ but not MNoV^{CW3}. Recently, we showed that MNoV^{CR6} infects rare IECs called tuft cells (30). To test whether tuft cells were essential for MNoV infection, we crossed *CD300lf*$^{F/F}$ mice to a double cortin-like kinase 1 (Dclk1) Cre—specific to tuft cells—to ablate CD300lf infection on tuft cells (46). We then infected *CD300lf*$^{F/F}$ *Dclk1Cre*− and *Cre*+ mice with 10^6 PFU PO of MNoV^{CR6}, MNoV^{CW3}, and chimeric MNoV^{CW3} expressing the NS1 of MNoV^{CR6} (MNoV$^{CW3\text{-}NS1\text{-}CR6}$). Mice were then sacrificed at 7 dpi for tissue analysis. Consistent with the *CD300lf*$^{F/F}$ *Vil1Cre* mice, MNoV^{CR6} was able to infect *CD300lf*$^{F/F}$ *Dclk1Cre*− mice but failed to infect *CD300lf*$^{F/F}$ *Dclk1Cre*+ animals, confirming that tuft cells are the exclusive site for MNoV^{CR6} infection (Fig. 2A to D). Both *CD300lf*$^{F/F}$

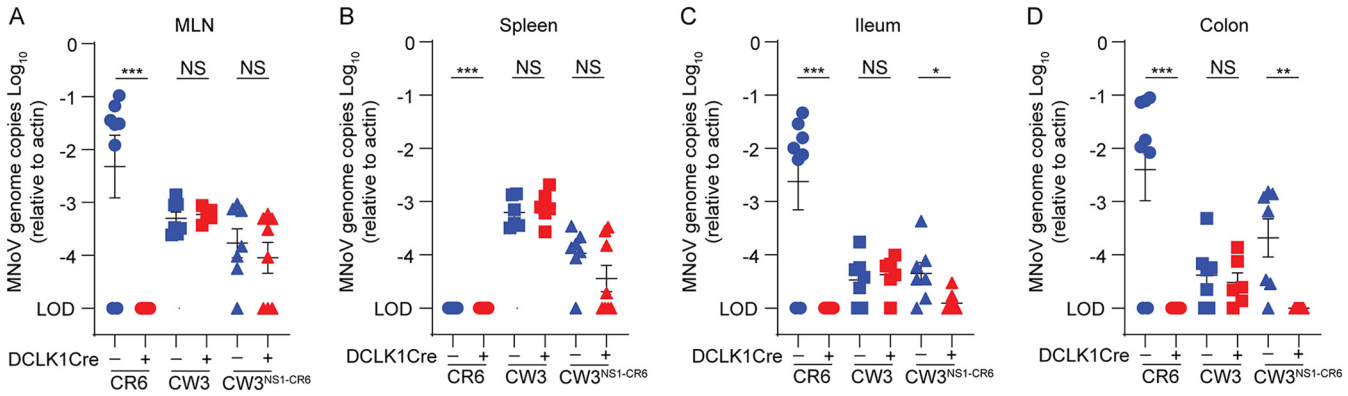

FIG 2 CD300lf expression on tuft cells is required for MNoV^{CR6} but not MNoV^{CW3} or MNoV$^{CW3\text{-}NS1\text{-}CR6}$ infection. *CD300lf$^{F/F}$ DCLK1Cre*− and *Cre*+ mice were infected with 10^6 PFU PO of MNoV^{CR6}, MNoV^{CW3}, and MNoV$^{CW3\text{-}NS1\text{-}CR6}$ and sacrificed at 7 dpi to assess viral titers in the MLN (A), spleen (B), ileum (C), and colon (D) by qPCR. MNoV genome copies were then normalized to actin. At least two independent repeats were performed using littermate controls. Statistical analysis was performed using Mann-Whitney test. Significance is annotated as follows: ***, $P < 0.001$; **, $P < 0.01$; *, $P < 0.05$; NS, not significant.

Dclk1Cre− and *Cre*+ were susceptible to MNoV^{CW3,} suggesting that CD300lf expression on tuft cells is not essential for MNoV^{CW3} infection (Fig. 2A to D). Interestingly, CD300lf disruption on tuft cells reduced MNoV$^{CW3\text{-}NS1\text{-}CR6}$ viral loads in the intestinal tissue but did not have a significant effect on MNoV$^{CW3\text{-}NS1\text{-}CR6}$ infection in systemic tissues (Fig. 2A to D). This result is consistent with the NS1 of MNoV^{CR6} enabling tuft cell tropism and the VP1 of MNoV^{CW3} promoting systemic infection (21, 25, 26, 32).

CD300lf expression on B cells and dendritic cells is not required for MNoV^{CW3} infection. We next evaluated the role of CD300lf-expressing hematopoietic cell types previously implicated in MNoV^{CW3} infection. B cells have been suggested as a target cell of both HuNoV and nonpersistent MNV both *in vivo* and *in vitro* (10, 43, 47). To test whether B cells were essential for MNoV^{CW3} infection, we generated a *CD300lf$^{F/F}$ CD19 Cre* line (48). CD19 is only transcribed in cells of the B cell lineage and is expressed throughout B cell development and differentiation. A total of 10^6 PFU of MNoV^{CW3} was administered PO to these mice, and tissue samples were harvested at 7 dpi for qPCR (Fig. 3). There was no significant difference in viral genomes between *CD300lf$^{F/F}$ CD19 Cre*+ and *Cre*− littermates, indicating that CD300lf on B cells is not essential for productive MNoV^{CW3} infection at 7 dpi (Fig. 3A to D).

As dendritic cells have also been implicated as a target cell of nonpersistent MNoV^{CW3} (43, 47, 49), we generated *CD300lf$^{F/F}$ CD11cCre* mice to test the role of dendritic cell infection in MNoV^{CW3} pathogenesis. CD11c, also known as integrin αX, is a widely used marker for dendritic cells (50). Similar to CD19-Cre, there was no significant difference in MNoV^{CW3} viral genome copies in the MLN, spleen, ileum, or colon (Fig. 3E to H), suggesting CD300lf expression on dendritic cells is not essential for productive MNoV^{CW3} infection *in vivo*.

CD300lf on LysM+ cells contribute to MNoV^{CW3} infection. To ascertain whether myelomonocytic cells were essential for MNoV^{CW3} infection, we generated mice with myeloid lineage cells deficient in CD300lf (*CD300lf$^{F/F}$ LysM Cre*). LysM is a lysozyme that is widely produced by immune cells and serves as a marker for myelomonocytic cells (51, 52). CD300lf expression on WT bone marrow macrophages (BMDMs) is below the limit of detection by flow cytometry (27). Therefore, we validated the activity of the Cre recombinase by harvesting BMDMs from both *CD300lf$^{F/F}$ LysM Cre*− and *Cre*+ mice and infecting these cells with MNoV^{CW3} at a multiplicity of infection (MOI) of 0.05. We quantified viral replication by plaque assay at 1- and 24-h postinfection (hpi). BMDMs from *CD300lf$^{F/F}$ LysM Cre*+ mice have reduced infectious virus compared to BMDMs from *LysM Cre*− littermates at 24 hpi, consistent with efficient CD300lf disruption in macrophages (Fig. 4A). *CD300lf$^{F/F}$ LysM Cre*− and *Cre*+ mice were then challenged with 10^6 PFU MNoV^{CW3} PO, and tissues were harvested at 7 dpi for qPCR. There was a significant reduction in viral genomes in spleen and ileum in *CD300lf$^{F/F}$ LysM*

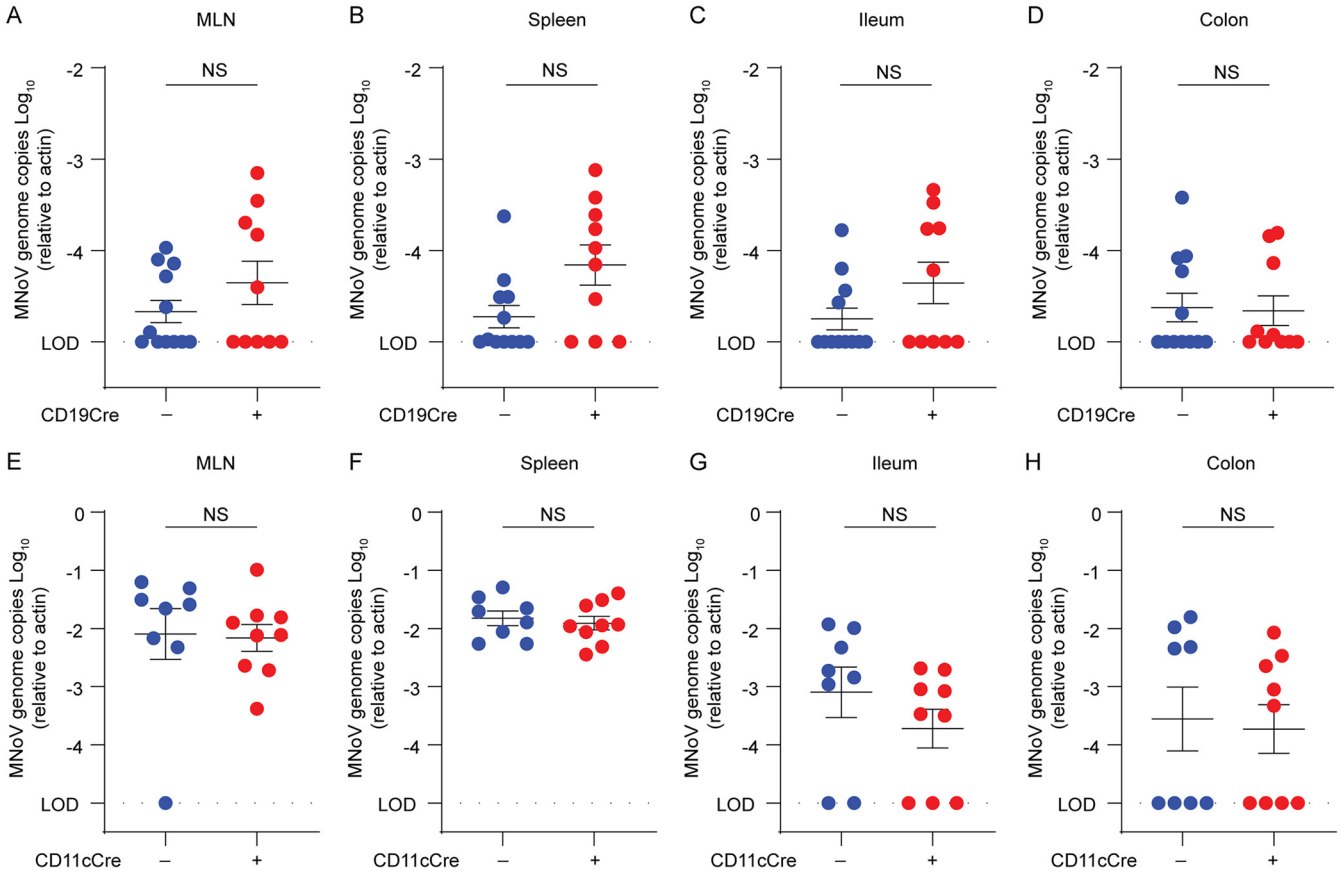

FIG 3 CD300lf expression on B cells (*CD19 Cre*+) and dendritic cells (*CD11c Cre*+) is not essential for MNoV^{CW3} infection *in vivo*. *CD300lf$^{F/F}$ CD19Cre* and *CD300lf$^{F/F}$ CD11cCre* mice were perorally infected with 10^6 PFU of MNoV^{CW3} and sacrificed at 7 dpi. MNoV titers in the MLN (A), spleen (B), ileum (C), and colon (D) of CD19 Cre mice were analyzed via qPCR for MNoV genome copies and normalized to actin. MNoV titers from the MLN (E), spleen (F), ileum (G), and colon (H) of CD11c Cre mice were analyzed by qPCR for viral genome copies and normalized to actin. Mouse experiments were performed using littermate controls with data pooled from four independent repeats. Data were analyzed via Mann-Whitney test. Statistical significance annotated as follows: NS, not significant.

Cre+ mice (Fig. 4B to E), suggesting that MNoV^{CW3} infection is in part supported by LysM+ cells *in vivo*. Interestingly, no significant difference in viral genomes was detected between *CD300lf$^{F/F}$ LysMCre*− and *Cre*+ littermates in the MLN and colon.

CD300lf expression on neutrophils is not essential for MNoV^{CW3} infection. LysM is expressed on macrophages and neutrophils, which both express CD300lf (27, 53, 54). To determine whether neutrophils are infected by MNoV^{CW3}, we crossed the *CD300lf$^{F/F}$* to a myeloid-related protein 8 (Mrp8) Cre mouse to generate mice with CD300lf-deficient neutrophils (*CD300lf$^{F/F}$ Mrp8 Cre*+). Blood samples were collected from these mice, and CD300lf disruption efficiency was assessed by flow cytometry (Fig. 5A). Samples harvested from *CD300lf$^{F/F}$ Mrp8 Cre*+ mice showed a reduction in CD300lf on neutrophils compared with that of the *CD300lf$^{F/F}$ Mrp8 Cre*− mice (Fig. 5B and C), confirming activity of the Cre recombinase. These mice were then infected PO with 10^6 PFU of MNoV^{CW3}, and tissues were collected at 7 dpi (Fig. 5D to G). Viral genome copies in the MLN, spleen, ileum, and colon were equivalent between *CD300lf$^{F/F}$ Mrp8 Cre*− and *Cre*+ mice (Fig. 5D to G). These results suggest that neutrophils are not required for MNoV^{CW3} infection *in vivo*.

CD300lf on LysM+ but not B cells contribute to MNoV^{CW3} infection during early infection. Next, we asked whether the cell tropism of MNoV^{CW3} varied across the course of acute infection. We evaluated the role of both CD19$^+$ and LysM+ cells in MNoV^{CW3} infection at 24 hpi. *CD300lf$^{F/F}$ CD19 Cre*+ mice were challenged with 10^6 PFU PO MNoV^{CW3}, and infectious virus was quantified in the MLN, spleen, ileum, and colon at 24 hpi by plaque assay (Fig. 6A to D). There were no significant differences in

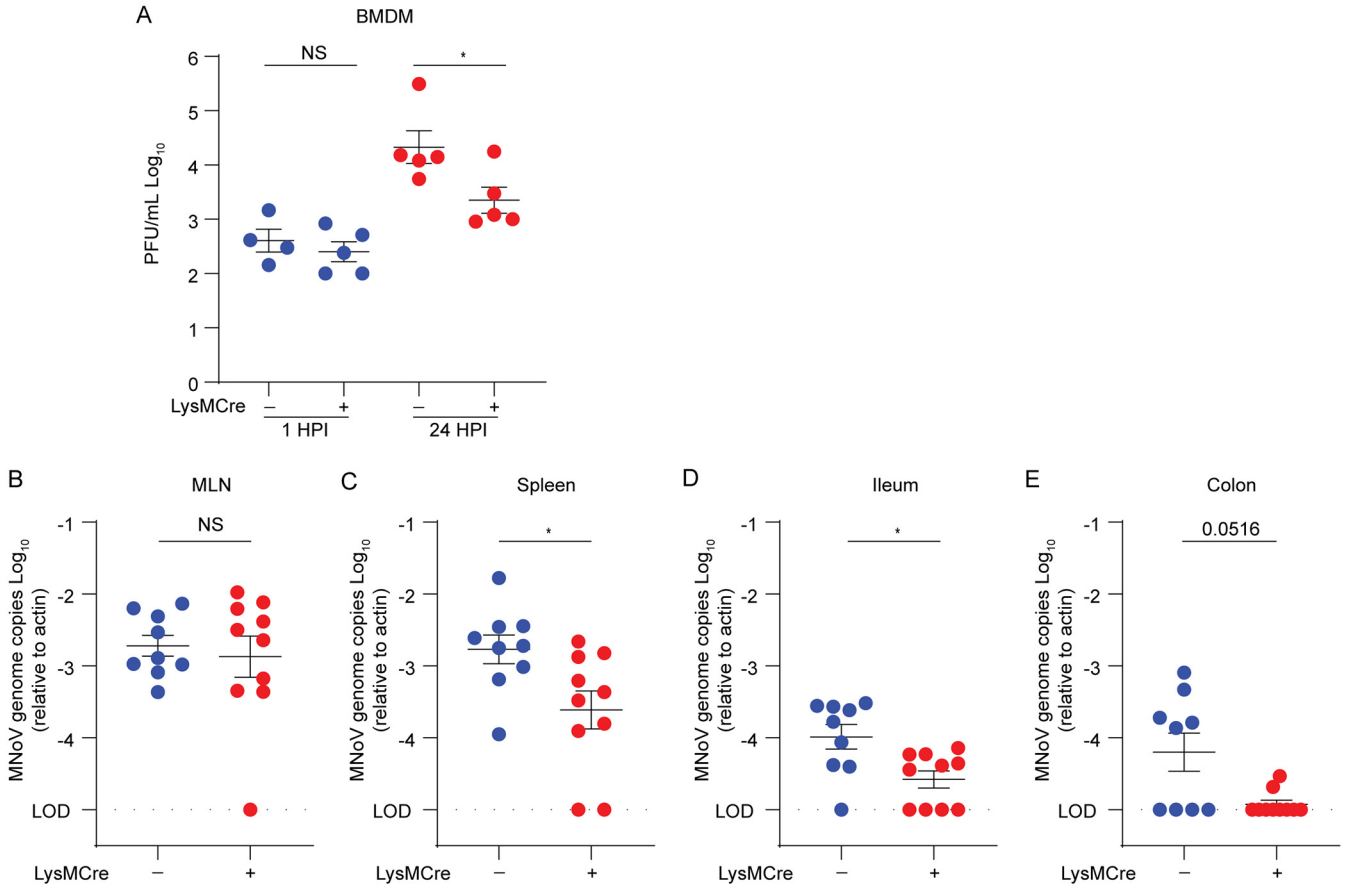

FIG 4 LysM+ cells contribute to productive MNoV^{CW3} infection in a CD300lf-dependent manner. (A) Bone marrow-derived macrophages from *CD300lf$^{F/F}$ LysMCre− and +* mice were infected with MNoV^{CW3} at an MOI of 0.05 for 1 or 24 hpi. Infectious virus was quantified by plaque assay. (B to E) *CD300lf$^{F/F}$ LysMCre* mice were perorally infected with 10^6 PFU of MNoV^{CW3} and sacrificed at 7 dpi. Tissue titers for the MLN (B), spleen (C), ileum (D), colon (E) were analyzed via qPCR for MNoV genome copies and normalized to actin. Mouse experiments were performed using littermate controls with four independent repeats analyzed via Mann-Whitney test. Data in A were analyzed via unpaired Student's *t* test. Statistical significance annotated as follows: *, $P < 0.05$; NS = not significant.

infectious virus between CD19 Cre− and Cre+ mice in any of the four tissues assessed, which is consistent with that observed at 7 dpi (Fig. 3). Notably, viral loads in the spleen are minimal at 24 hpi, which is consistent with the known kinetics of dissemination of MNoV^{CW3} to the spleen (25). Next, we infected *CD300lf$^{F/F}$ LysM Cre−* and *Cre+* mice with 10^6 PFU PO MNoV^{CW3} and quantified infectious virus in the MLN, spleen, ileum, and colon at 24 hpi by plaque assay (Fig. 6D to H). *LysM Cre+* mice exhibited reduced virus in the ileum at 24 hpi, consistent with that observed at 7 dpi (Fig. 4). Infectious virus was detected similar levels between *LysM Cre− and LysM Cre+* mice in the MLN, spleen, and colon.

MNoV^{CW3} infection of LysM+ cells is not essential for lethality in innate immune-deficient mice. Mice deficient in type I interferon signaling, including *Stat1$^{-/-}$*, mice are highly susceptible to MNoV^{CW3} infection resulting in lethality (23, 45). Given that LysM+ cells contribute to MNoV^{CW3} infection, we asked whether disruption of CD300lf on LysM+ cells would confer protection against MNoV^{CW3} on a *Stat1$^{-/-}$* background. We challenged *CD300lf$^{F/F}$ LysMCre− Stat1$^{-/-}$* or *Cre+ Stat1$^{-/-}$* mice with 10^4 or 10^6 PFU MNoV^{CW3} and assessed survival. No significant differences in lethality were observed between these groups at either viral challenge dose (Fig. 7A and B). Next, we harvested tissues for viral RNA quantification at 3 dpi, prior to the onset of lethality. Interestingly, viral genomes were equivalent between the *CD300lf$^{F/F}$ LysM Cre− Stat$^{-/-}$* and *CD300lf$^{F/F}$ LysM Cre+ Stat$^{-/-}$* mice across tissues (Fig. 7C to F). These results indicate that in the absence of STAT1 signaling, MNoV^{CW3} infection is not dependent on the expression of CD300lf on LysM+ cells.

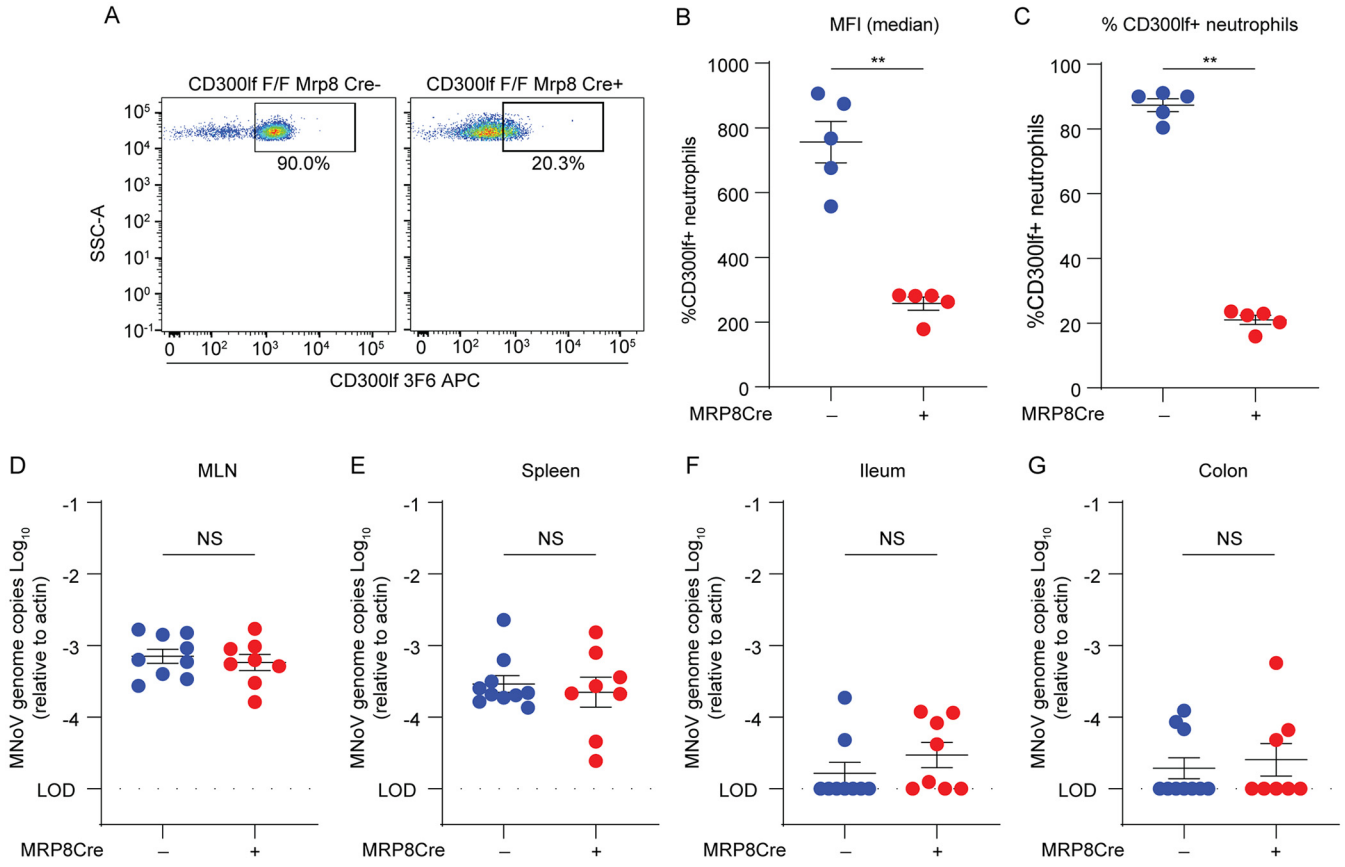

FIG 5 CD300lf depletion on neutrophils does not affect MNoV^{CW3} infection *in vivo*. (A) FACS plot and quantification of CD300lf expression levels on neutrophils harvested from *CD300lf$^{F/F}$ MRP8 Cre* mice. Each dot represents one mouse. (B) Mean fluorescent intensity (MFI) of CD300lf expression on neutrophils. (C) Detection of CD300lf+ neutrophils in *CD300lf$^{F/F}$ MRP8* Cre− and *CD300lf$^{F/F}$ MRP8* Cre+ mice. *CD300lf$^{F/F}$ MRP8Cre* mice were infected with 10^6 PFU PO of MNoV^{CW3} and sacrificed at 7 dpi. MNoV^{CW3} genome copies from MLN (D), spleen (E), ileum (F), and colon (G) were analyzed by qPCR and normalized to actin. Data in A to C were analyzed via Mann-Whitney test and are representative of at least two independent experiments. Mouse experiments were performed using littermate controls with two independent repeats analyzed via Mann-Whitney test. Statistical significance annotated as follows: **, $P < 0.01$; NS, not significant.

DISCUSSION

We previously identified CD300lf as the primary physiologic receptor for MNoV (27, 30). CD300lf is necessary and sufficient for infection of diverse MNoV strains *in vivo* which we leveraged to interrogate MNoV cell tropism (27, 30). Here, we introduce a novel conditional knockout mouse model that serves as a valuable tool for studying tissue-specific CD300lf expression. We previously demonstrated that persistent MNoV^{CR6} infects a rare population of IECs called tuft cells. However, it was unknown whether tuft cell infection is essential *in vivo*, as other putative target cells may support MNoV^{CR6} replication. Here, we show that that MNoV^{CR6} infection can be ablated by conditionally deleting CD300lf on IECs broadly and tuft cells more specifically. This result demonstrates that CD300lf expression on tuft cells is essential for oral infection of MNoV^{CR6}. In contrast to MNoV^{CR6}, MNoV^{CW3} was unaffected by conditional ablation of CD300lf on both IECs and tuft cells. Using a chimeric virus (MNoV$^{CW3\text{-}NS1\text{-}CR6}$), we demonstrated that the NS1 of CR6 permits tuft cell tropism, which requires tuft cell-specific CD300lf expression for intestinal tissue infection (21, 25, 30, 32). Interestingly, MNoV$^{CW3\text{-}NS1\text{-}CR6}$ maintained the ability to infect systemic tissues, suggesting additional determinants of cell and tissue tropism for MNoV. These data ultimately support different tropism patterns across MNoV strains.

Previous reports identified dendritic cells, B cells, macrophages, monocytes, and neutrophils as targets of MNoV^{CW310} (42, 44, 47). We therefore sought to investigate the relative contribution of these cell types to MNoV^{CW3} infection by crossing *CD300lf$^{F/F}$*

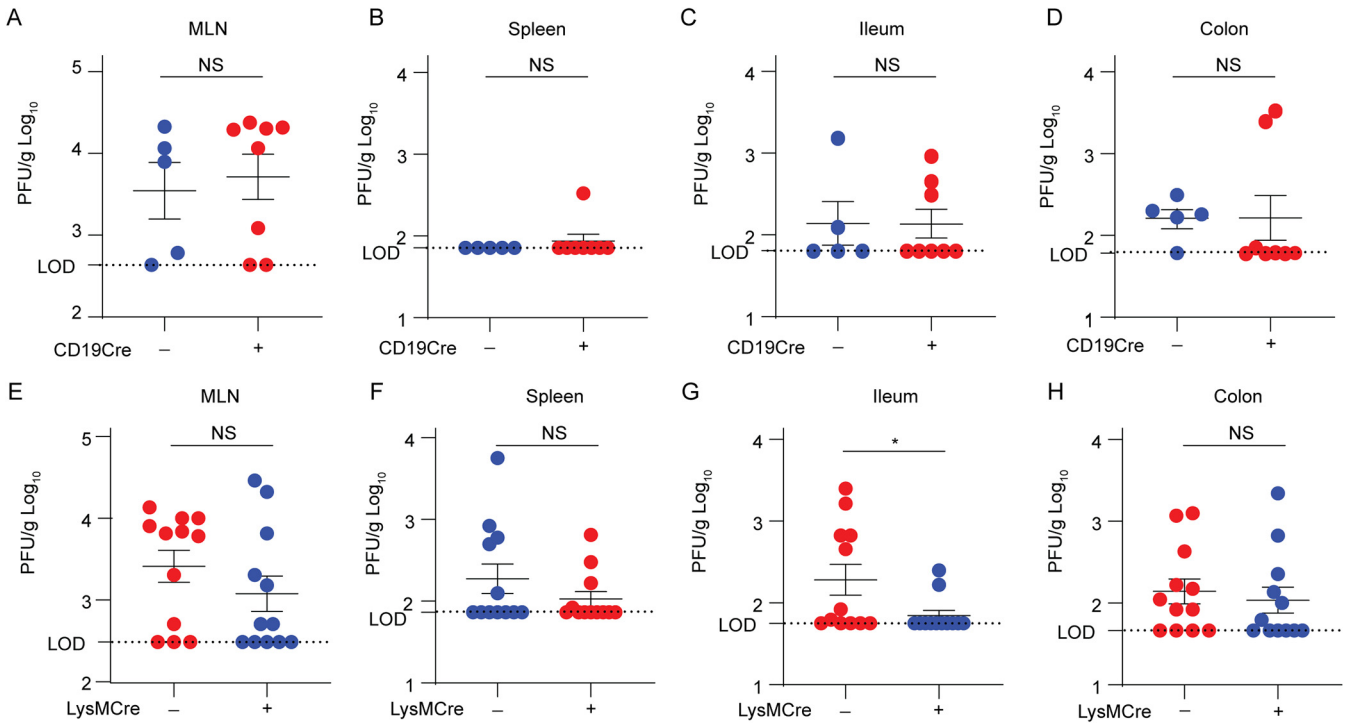

FIG 6 CD300lf deletion from LysM+ but not B cells reduces intestinal MNoV^{CW3} at 24 hpi. (A) *CD300lf$^{F/F}$ CD19 Cre* mice were infected PO with 10^6 PFU MNoV^{CW3}. Infectious virus was quantified by plaque assay at 24 hpi in the MLN (A), spleen (B), ileum (C), and colon (D). Data are shown as PFU per gram of tissue. *CD300lf$^{F/F}$ LysMCre* mice were infected PO with 10^6 PFU of MNoV^{CW3} and sacrificed at 24 hpi. Infectious virus was quantified by plaque assay in the MLN (E), spleen (F), ileum (G), and colon (H). Data are pooled from at least two independent experiments, each performed with littermate controls. Data were analyzed by Mann-Whitney test. Statistical significance annotated as follows: *, $P < 0.05$; NS, not significant.

mice to cell-specific Cre recombinases to generate mouse lines with CD300lf deleted on specific target cells. We demonstrated that CD300lf expression on LysM+ cells (i.e., macrophages and monocytes) significantly contributes to MNoV^{CW3} infection, whereas we observed no impact of CD300lf disruption on dendritic cells, B cells, and neutrophils. Our finding that LysM+ cells are important for MNoV^{CW3} infection is consistent with a recent report demonstrating that MNoV^{CW3} requires susceptible myeloid cells and depends on cell lysis to induce chemotaxis and inflammatory responses for myeloid cell recruitment to the site of infection (44). Our observation of only a partial reduction in MNoV^{CW3} viral load in mice in which CD300lf is ablated from LysM+ cells supports that a single target cell type may not be essential for MNoV^{CW3} infection, as it is for MNoV^{CR6}. Instead, multiple CD300lf-expressing cell types likely contribute to infection and pathogenesis. Alternatively, it is possible that the lack of complete resistance to MNoV^{CW3} in any of the seven Cre lines tested may result from incomplete Cre-mediated recombination of MNoV^{CW3} target cells or infection of an as yet unidentified cell type.

MNoV tropism is governed both by virus-receptor and virus-immune system interactions. Specifically, disruption of type I IFN signaling through *Ifnar* or *Stat1* deletion results in lethal MNoV^{CW3} infection and systemic spread of MNoV^{CR6} likely due to expanded cell tropism (23, 26). Consistent with this finding, we observed no reduction of MNoV^{CW3} viral load in *Stat1*$^{-/-}$ mice with conditional ablation of CD300lf on LysM+ cells, demonstrating that STAT1 partially restricts MNoV^{CW3} to myelomonocytic cells, and suggests an expanded tropism in mice lacking innate immunity. The mechanisms of this restriction represent an important area of future investigation.

In addition to its role in MNoV infection, CD300lf has been implicated in diverse disease states, including multiple sclerosis, inflammatory bowel disease, and depression (34, 36–38, 55). Elucidating the cell type-specific role of CD300lf in these disease contexts may provide critical insight into mechanisms of pathogenesis. The mouse model

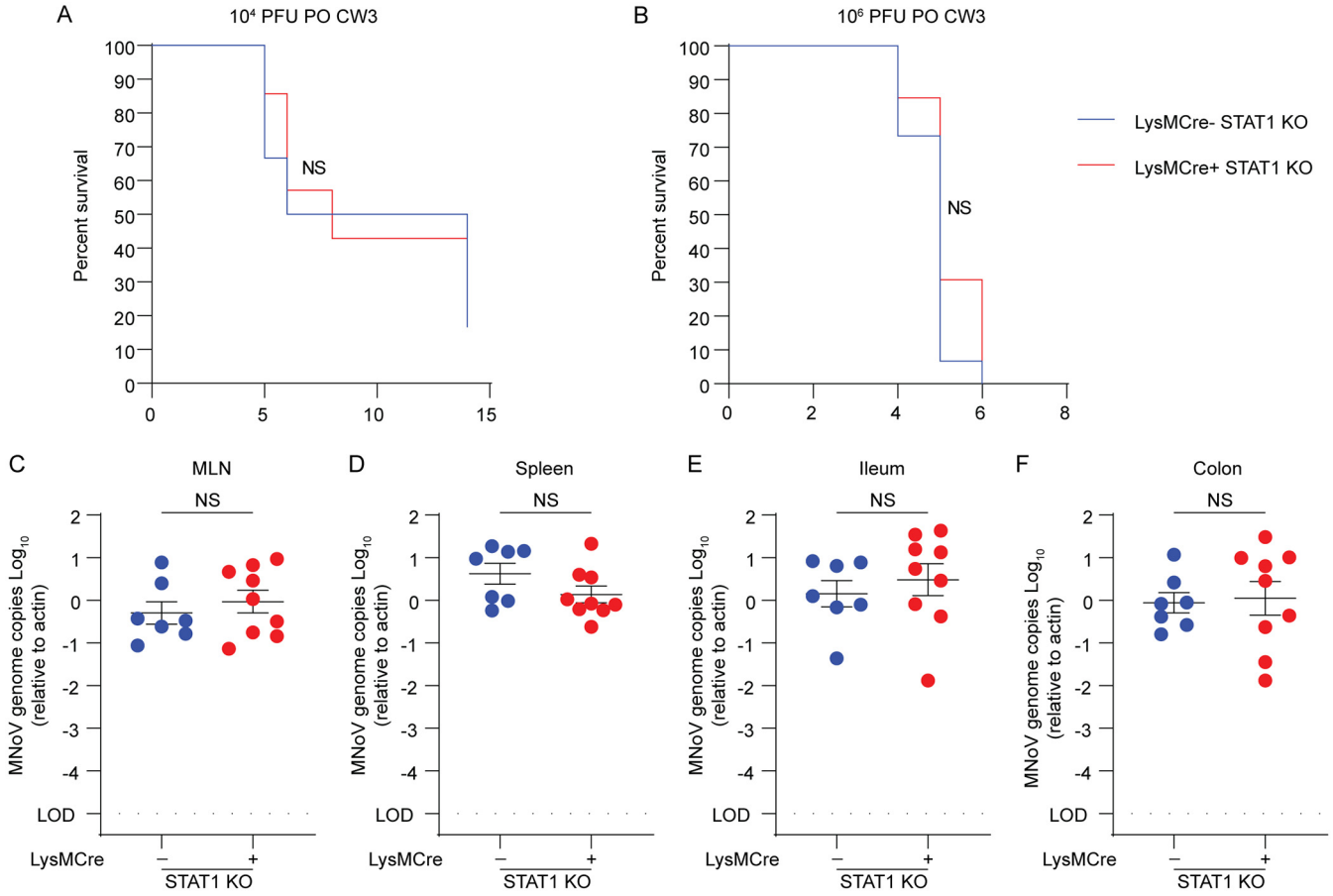

FIG 7 Ablation of CD300lf expression on LysM$^+$ cells does not provide protection from lethal MNoV^{CW3} infection in *Stat1*$^{-/-}$ mice. (A and B) *CD300lf*$^{F/F}$ *LysMCre* × *Stat1*$^{-/-}$mice were infected with either 10^4 (A) or 10^6 (B) PFU of MNoV^{CW3} and monitored for lethality. (C to F) *CD300lf*$^{F/F}$ *LysMCre* mice were infected with 10^6 PFU PO of MNoV^{CW3} and sacrificed at 3 dpi. Tissue titers for the MLN (C), spleen (D), ileum (E), and colon (F) were analyzed via qPCR for MNoV genome copies and normalized to actin. Mouse experiments were performed using littermate controls with pooled data from at least two independent experiments and analyzed via Mann-Whitney test. Kaplan-Meier curves were generated for survival experiments. Statistical significance annotated as follows: NS, not significant.

described here thus provides an important tool for studying CD300lf expression in various contexts.

HuNoV cell tropism remains incompletely understood. Diverse hematopoietic and epithelial cell types, including enteroendocrine cells, have been implicated in HNoV infection *in vivo* in humans, nonnative hosts, and *in vitro* (6, 8, 9, 11, 18). Elucidating the host and viral determinants governing HNoV tropism may reveal insight into HNoV transmission, pathogenesis, and persistence. MNoV provides a useful tool to reveal molecular interactions at the viral and host levels that may inform studies of HNoV. Here, we demonstrate that subtle genetic variation among MNoV strains can result in substantial differences in cell tropism. This suggests a similar phenomenon may be at play for HNoV.

MATERIALS AND METHODS

Mouse strains. Cd300lf conditional knockout mice were generated by introducing LoxP sites flanking exon 3 of Cd300lf. The 5′ and 3′ LoxP sites were introduced by CRISPR/Cas9-mediated homology-directed repair. The following single guide RNAs (sgRNAs) were used: GTGTTGTGGCCTAACTTGCANGG and TCAAGTTCCCTGTCTCTTGGGGG to insert donor sequences GAATTCATAACTTCGTATAATGTATGCTA TACGAAGTTAT at Chr11 (nucleotides 115,122,845 to 115,122,846) and GTGCTCATTAATGATGTTC TCTTTGAGAGTCCTTCTAGAG at Chr11 (nucleotides 115,125,303 to 115,125,304), respectively. Mice were genotyped by qPCR for the 5′ LoxP site at Transnetyx, Inc.

Ethics statement. Animal use and care was approved in agreement with the Yale Animal Resource Center and Institution Animal Care and Use Committee (number 2018-20198) according to the standards set by the Animal Welfare Act.

Viral stocks. Molecular clones of MNoV^{CW3} (Gen Bank accession EF014462.1) and MNoV^{CR6} (Gen Bank accession JQ237823) were used to generate a working stock of infectious virus. To create stocks, plasmids containing infectious molecular clones were transfected into 293T cells (ATCC) to generate a P0 stock as described previously (26, 27). Then, the P0 stock was used to infect susceptible BV2 cells (gifted from H.W. Virgin) for generation of the P1 stock. Generation of the P2 stock was performed by inoculating BV2 cells with the P1 stock for 48 hours followed by freezing/thawing the infected cultures at –80°C. Upon thawing the infected BV2 cultures, cellular debris was pelleted at 1,200 $\times$ *g* for 5 minutes and then filtered through a 0.22-μm filter. Viral stocks were aliquoted and stored at –80°C. Virus titer was determined by plaque assay at least three independent times.

Cell culture. BV2 cells were maintained in Dulbecco's modified Eagle media (DMEM; Gibco, Gaithersburg, MD) was supplemented with 10% fetal bovine serum (FBS; VWR, Radnor, PA), 1% HEPES (Gibco), and 1% penicillin/streptomycin (pen/strep; Gibco). In order to differentiate bone marrow progenitors into BMDMs, 10^6 cells were plated into a 10-cm nontissue culture plate with BMDM media (DMEM, 10% FBS, 10% CMG14 conditioned media, 2 mM L-glutamine, 1% pen/strep, and 1% sodium pyruvate), incubated at 37°C for 7 days at 5% CO_2 (56). Differentiation of progenitors into BMDMs was confirmed by assessing F4/80 expression by flow cytometry. More than 95% of cells were F4/80+.

***In vitro* MNoV infections.** BMDMs from *Cd300lf*$^{-/-}$ and *Cd300lf*$^{f/f}$ *LysMCre* mice were generated as described above. After 7 days in differentiation media, 50,000 cells were plated per well of a 96-well plate and infected with MNoV^{CW3} at an MOI of 0.05. Infected plates were frozen at –80°C at 1 and 24 hpi for plaque assay.

***In vivo* MNoV infections.** Trio breeding (one male and two females) was used to generate mice for experiments. Littermate controls were used for all experiments. Mouse infections were performed by inoculating mice with 25 μl of 10^6 PFU MNoV^{CW3} or MNoV^{CR6} diluted in DMEM supplemented with 10% FBS. At 1 or 7 dpi, mice were sacrificed by isoflurane overdose. Freshly collected fecal pellets and approximately 20 mg of MLN, spleen, small intestine, and proximal colon were collected and flash frozen for qPCR analysis. For plaque assay, MLN, spleen, 10 cm of central small intestine (ileum), and the entire colon were collected and weighed prior to flash freezing in 1 ml of DMEM supplemented with 10% FBS, 1% pen/strep, and 1% HEPES. Tissue and fecal samples as well as tissues were stored at –80°C until processing. Immediately before quantification of virus by plaque assay, tissues were thawed and homogenized with 1.0-mm silica beads.

Viral quantification by plaque assay. Each well of a 6-well plate was seeded with 1.8×10^6 BV2 cells in DMEM with 10% FBS, 1% pen/strep, and 1% HEPES and then incubated overnight at 37°C and 5% CO_2. After 24 h, the BV2 cells were checked for confluence, and BMDM-infected plates were thawed, followed by 6 serial dilutions. The medium was removed from the BV2 cells, and one diluted inoculum was added to one well of the 6-well plate and rocked gently for 1 hour. After rocking, the inoculum was removed, and 2 ml overlay medium was applied (MEM with 10% FBS containing 1% methylcellulose, 1% HEPES, 1% GlutaMAX [Gibco], and 1% pen/strep) followed by a 48-h incubation. Following incubation, the overlay medium was aspirated off and each well was stained with 1 ml crystal violet (20% ethanol and 0.2% [wt/vol] crystal violet) on a plate rocker for 30 min as previously described (27).

Quantitative PCR. Viral genome copies in tissues and fecal pellets were previously described (27, 30). Briefly, viral RNA extraction from tissues was performed using TRIzol (Life Technologies, Carlsbad, CA) and purified with a Direct-zol RNA miniprep plus kit according to the manufacturer's protocol (Zymo Research, Irvine, CA). Following purification, a two-step cDNA synthesis was performed using 5 μl of RNA and random hexamers, and ImProm-II reverse transcriptase (Promega) was performed. qPCR analysis on standard curves and samples was performed in duplicate using MNoV-specific oligonucleotides, as follows: forward primer, 5′-CACGCCACCGATCTGTTCTG-3′; reverse primer, 5′-GCGCTGCGCCATCACTC-3′; and probe, 5′-6-carboxyfluorescein [FAM]-CGCTTTGGAACAATG-MGBNFQ-3′. The limit of detection for qPCR analysis was 10 MNoV genome copies/1 μl. MNoV genome copies were normalized to the expression of housekeeping gene β-actin detected using the following: forward primer, 5′-GCTCC TTCGTTGCCGTCCA-3′; reverse primer, 5′-TTGCACATGCCGGAGCCGTT-3′; and probe, 5′-6-JOE (6-carboxy-4′,5′-dichloro-2′,7′-dimethoxyfluorescein NHS ester)-CACCAGTTC/ZEN/GCCATGGATGACGA-IABKFQ (Iowa Black FQ quencher)-3′. The limit of detection for β-actin was 100 copies/1 μl. Undetectable genome copies were set at 0.0001 copies relative to actin.

Tissue processing and low cytometry. Mice were euthanized and sacrificed in compliance with the IACUC protocol. Colonic tissue was harvested, opened longitudinally, and washed three times in ice cold 1$\times$ Dulbecco's PBS (DPBS). To dissociate cells, colonic tissue was finely chopped with a razor blade and suspended in stripping buffer (1$\times$ DPBS, 5% FBS, 0.1% pen/strep, 5 mM EDTA, and 0.5 M dithiothreitol [DTT]). Cells were incubated at 37°C for 15 min and gently agitated at 200 rpm. Dissociated cells were filtered sequentially through 100-μm filters and then through 40-μm filters. Cellular filtrate was pelleted by centrifugation (1,500 rpm for 5 min at 4°C) and washed once with fluorescence-activated cell sorter (FACS) buffer (1$\times$ DPBS, 2 mM EDTA, and 2.5% FBS). Cells were then stained for viability with Zombie Aqua (BioLegend) diluted 1:500 in 1$\times$ DPBS on ice for 10 min. Samples were centrifuged at 1,200 $\times$ *g* for 2 min, and the supernatant was removed. CD300lf primary antibody 3F6 (Armenian hamster; Genentech) was added at a 1:800 dilution for 20 min at room temperature (38). Cells were then washed with FACS buffer. To identify epithelial cells expressing CD300lf, cells were stained with the following antibodies diluted in FACS buffer: Alexa Fluor 488 goat anti-Armenian hamster (1:500; 127545160; lot 128099; in 50% glycerol; Jackson ImmunoResearch), EpCAM (1:200; BioLegend), SiglecF (1:200; BioLegend), CD24 (1:200; BioLegend), and CD45 (1:200; BioLegend) on ice for 20 min. Cells were washed with FACS buffer, resuspended in 4% paraformaldehyde, and filtered. Samples were analyzed on a CytoFLEX S instrument (Beckman Coulter).

Statistical analysis. Statistical analysis was performed in Prism GraphPad version 8 (San Diego, CA). Error bars show the standard error of the mean unless indicated otherwise. For all nonnormally distributed data, Mann-Whitney tests were performed, whereas normally distributed data were analyzed with an unpaired Student's *t* test. Kaplan-Meier curves were used to analyze survival data. *P* values of <0.05 were considered significant (*, $P < 0.05$; **, $P < 0.01$; ***, $P < 0.001$; ****, $P < 0.0001$).

Data availability. All relevant data are contained within the manuscript. *CD300lf*$^{F/F}$ mice are available upon request.

ACKNOWLEDGMENTS

We acknowledge Herbert "Skip" Virgin, Michael White, Shondra Pruett-Miller, and Darren Kreamalmayer for their generous resources, guidance, and technical support. We thank Timothy Wang for sharing critical reagents and the Washington University Genome Engineering and iPSC Center for genetically engineering mice.

This work was supported by the Burroughs Wellcome Fund (C.B.W.); NSF DGE1752134 (M.S.S.); and NIH grants K08 A1128043 (C.B.W.), R01 AI148467 (C.B.W.), ROO Dk116666 (R.C.O.), R01 AI127552 (M.T.B.), and R01 AI139314 (M.T.B.).

V.R.G., conceptualization, formal analysis, investigation, writing—original draft, and visualization; M.M.A., validation, formal analysis, investigation, writing—original draft, and visualization; C.O.S., formal analysis and investigation; R.B.F., investigation; M.S.S., formal analysis and investigation; J.W., investigation; L.L.H., investigation; M.T.B., conceptualization and supervision; T.J.N., conceptualization and supervision; S.L., conceptualization and supervision; R.C.O., conceptualization, methodology, supervision, and resources; C.B.W., conceptualization, methodology, supervision, investigation, resources, funding acquisition, and writing—original draft. All authors reviewed and edited the manuscript.

REFERENCES

1. Patel MM, Widdowson MA, Glass RI, Akazawa K, Vinjé J, Parashar UD. 2008. Systematic literature review of role of noroviruses in sporadic gastroenteritis. Emerg Infect Dis 14:1224–1231. https://doi.org/10.3201/eid1408.071114.
2. Ahmed SM, Hall AJ, Robinson AE, Verhoef L, Premkumar P, Parashar UD, Koopmans M, Lopman BA. 2014. Global prevalence of norovirus in cases of gastroenteritis: a systematic review and meta-analysis. Lancet Infect Dis 14:725–730. https://doi.org/10.1016/S1473-3099(14)70767-4.
3. Kroneman A, Vega E, Vennema H, Vinjé J, White PA, Hansman G, Green K, Martella V, Katayama K, Koopmans M. 2013. Proposal for a unified norovirus nomenclature and genotyping. Arch Virol 158:2059–2068. https://doi.org/10.1007/s00705-013-1708-5.
4. Karst SM, Wobus CE, Goodfellow IG, Green KY, Virgin HW. 2014. Advances in norovirus biology. Cell Host Microbe 15:668–680. https://doi.org/10.1016/j.chom.2014.05.015.
5. Karst SM, Tibbetts SA. 2016. Recent advances in understanding norovirus pathogenesis. J Med Virol 88:1837–1843. https://doi.org/10.1002/jmv.24559.
6. Graziano VR, Wei J, Wilen CB. 2019. Norovirus attachment and entry. Viruses 11:495. https://doi.org/10.3390/v11060495.
7. Katayama K, Murakami K, Sharp TM, Guix S, Oka T, Takai-Todaka R, Nakanishi A, Crawford SE, Atmar RL, Estes MK. 2014. Plasmid-based human norovirus reverse genetics system produces reporter-tagged progeny virus containing infectious genomic RNA. Proc Natl Acad Sci U S A 111:E4043–E4052. https://doi.org/10.1073/pnas.1415096111.
8. Ettayebi K, Crawford SE, Murakami K, Broughman JR, Karandikar U, Tenge VR, Neill FH, Blutt SE, Zeng XL, Qu L, Kou B, Opekun AR, Burrin D, Graham DY, Ramani S, Atmar RL, Estes MK. 2016. Replication of human noroviruses in stem cell-derived human enteroids. Science 353:1387–1393. https://doi.org/10.1126/science.aaf5211.
9. Green KY, Kaufman SS, Nagata BM, Chaimongkol N, Kim DY, Levenson EA, Tin CM, Yardley AB, Johnson JA, Barletta ABF, Khan KM, Yazigi NA, Subramanian S, Moturi SR, Fishbein TM, Moore IN, Sosnovtsev SV. 2020. Human norovirus targets enteroendocrine epithelial cells in the small intestine. Nat Commun 11:2759. https://doi.org/10.1038/s41467-020-16491-3.
10. Jones MK, Watanabe M, Zhu S, Graves CL, Keyes LR, Grau KR, Gonzalez-Hernandez MB, Iovine NM, Wobus CE, Vinjé J, Tibbetts SA, Wallet SM, Karst SM. 2014. Enteric bacteria promote human and mouse norovirus infection of B cells. Science 346:755–759. https://doi.org/10.1126/science.1257147.
11. Jones MK, Grau KR, Costantini V, Kolawole AO, de Graaf M, Freiden P, Graves CL, Koopmans M, Wallet SM, Tibbetts SA, Schultz-Cherry S, Wobus CE, Vinjé J, Karst SM. 2015. Human norovirus culture in B cells. Nat Protoc 10:1939–1947. https://doi.org/10.1038/nprot.2015.121.
12. Davis A, Cortez V, Grodzki M, Dallas R, Ferrolino J, Freiden P, Maron G, Hakim H, Hayden RT, Tang L, Huys A, Kolawole AO, Wobus CE, Jones MK, Karst SM, Schultz-Cherry S. 2020. Infectious norovirus is chronically shed by immunocompromised pediatric hosts. Viruses 12:619. https://doi.org/10.3390/v12060619.
13. Bok K, Parra GI, Mitra T, Abente E, Shaver CK, Boon D, Engle R, Yu C, Kapikian AZ, Sosnovtsev SV, Purcell RH, Green KY. 2011. Chimpanzees as an animal model for human norovirus infection and vaccine development. Proc Natl Acad Sci U S A 108:325–330. https://doi.org/10.1073/pnas.1014577107.
14. Seo DJ, Jung D, Jung S, Ha SK, Ha SD, Choi IS, Myoung J, Choi C. 2018. Experimental miniature piglet model for the infection of human norovirus GII. J Med Virol 90:655–662. https://doi.org/10.1002/jmv.24991.
15. Taube S, Kolawole AO, Höhne M, Wilkinson JE, Handley SA, Perry JW, Thackray LB, Akkina R, Wobus CE. 2013. A mouse model for human norovirus. mBio 4:e00450-13. https://doi.org/10.1128/mBio.00450-13.
16. Cheetham S, Souza M, Meulia T, Grimes S, Han MG, Saif LJ. 2006. Pathogenesis of a genogroup II human norovirus in gnotobiotic pigs. J Virol 80:10372–10381. https://doi.org/10.1128/JVI.00809-06.
17. Jung K, Wang Q, Kim Y, Scheuer K, Zhang Z, Shen Q, Chang KO, Saif LJ. 2012. The effects of simvastatin or interferon-α on infectivity of human norovirus using a gnotobiotic pig model for the study of antivirals. PLoS One 7:e41619. https://doi.org/10.1371/journal.pone.0041619.
18. Karandikar UC, Crawford SE, Ajami NJ, Murakami K, Kou B, Ettayebi K, Papanicolaou GA, Jongwutiwes U, Perales MA, Shia J, Mercer D, Finegold MJ, Vinjé J, Atmar RL, Estes MK. 2016. Detection of human norovirus in intestinal biopsies from immunocompromised transplant patients. J Gen Virol 97:2291–2300. https://doi.org/10.1099/jgv.0.000545.
19. Murakami K, Tenge VR, Karandikar UC, Lin SC, Ramani S, Ettayebi K, Crawford SE, Zeng XL, Neill FH, Ayyar BV, Katayama K, Graham DY, Bieberich E, Atmar RL, Estes MK. 2020. Bile acids and ceramide overcome the entry restriction for GII.3 human norovirus replication in human

intestinal enteroids. Proc Natl Acad Sci U S A 117:1700–1710. https://doi.org/10.1073/pnas.1910138117.
20. Nelson CA, Wilen CB, Dai YN, Orchard RC, Kim AS, Stegeman RA, Hsieh LL, Smith TJ, Virgin HW, Fremont DH. 2018. Structural basis for murine norovirus engagement of bile acids and the CD300lf receptor. Proc Natl Acad Sci U S A 115:E9201–E9210. https://doi.org/10.1073/pnas.1805797115.
21. Lee S, Wilen CB, Orvedahl A, McCune BT, Kim KW, Orchard RC, Peterson ST, Nice TJ, Baldridge MT, Virgin HW. 2017. Norovirus cell tropism is determined by combinatorial action of a viral non-structural protein and host cytokine. Cell Host Microbe 22:449–459.e4. https://doi.org/10.1016/j.chom.2017.08.021.
22. Baldridge MT, Turula H, Wobus CE. 2016. Norovirus regulation by host and microbe. Trends Mol Med 22:1047–1059. https://doi.org/10.1016/j.molmed.2016.10.003.
23. Karst SM, Wobus CE, Lay M, Davidson J, Virgin HW, IV. 2003. STAT1-dependent innate immunity to a Norwalk-like virus. Science 299:1575–1578. https://doi.org/10.1126/science.1077905.
24. Wobus CE, Thackray LB, Virgin HW, IV. 2006. Murine norovirus: a model system to study norovirus biology and pathogenesis. J Virol 80:5104–5112. https://doi.org/10.1128/JVI.02346-05.
25. Nice TJ, Strong DW, McCune BT, Pohl CS, Virgin HW. 2013. A single-amino-acid change in murine norovirus NS1/2 is sufficient for colonic tropism and persistence. J Virol 87:327–334. https://doi.org/10.1128/JVI.01864-12.
26. Strong DW, Thackray LB, Smith TJ, Virgin HW. 2012. Protruding domain of capsid protein is necessary and sufficient to determine murine norovirus replication and pathogenesis in vivo. J Virol 86:2950–2958. https://doi.org/10.1128/JVI.07038-11.
27. Orchard RC, Wilen CB, Doench JG, Baldridge MT, McCune BT, Lee YC, Lee S, Pruett-Miller SM, Nelson CA, Fremont DH, Virgin HW. 2016. Discovery of a proteinaceous cellular receptor for a norovirus. Science 353:933–936. https://doi.org/10.1126/science.aaf1220.
28. Roth AN, Helm EW, Mirabelli C, Kirsche E, Smith JC, Eurell LB, Ghosh S, Altan-Bonnet N, Wobus CE, Karst SM. 2020. Norovirus infection causes acute self-resolving diarrhea in wild-type neonatal mice. Nat Commun 11:2968. https://doi.org/10.1038/s41467-020-16798-1.
29. Graziano VR, Walker FC, Kennedy EA, Wei J, Ettayebi K, Strine MS, Filler RB, Hassan E, Hsieh LL, Kim AS, Kolawole AO, Wobus CE, Lindesmith LC, Baric RS, Estes MK, Orchard RC, Baldridge MT, Wilen CB. 2020. CD300lf is the primary physiologic receptor of murine norovirus but not human norovirus. PLoS Pathog 16:e1008242. https://doi.org/10.1371/journal.ppat.1008242.
30. Wilen CB, Lee S, Hsieh LL, Orchard RC, Desai C, Hykes BL, McAllaster MR, Balce DR, Feehley T, Brestoff JR, Hickey CA, Yokoyama CC, Wang YT, MacDuff DA, Kreamalmayer D, Howitt MR, Neil JA, Cadwell K, Allen PM, Handley SA, van Lookeren Campagne M, Baldridge MT, Virgin HW. 2018. Tropism for tuft cells determines immune promotion of norovirus pathogenesis. Science 360:204–208. https://doi.org/10.1126/science.aar3799.
31. Robinson BA, Van Winkle JA, McCune BT, Peters AM, Nice TJ. 2019. Caspase-mediated cleavage of murine norovirus NS1/2 potentiates apoptosis and is required for persistent infection of intestinal epithelial cells. PLoS Pathog 15:e1007940. https://doi.org/10.1371/journal.ppat.1007940.
32. Lee S, Liu H, Wilen CB, Sychev ZE, Desai C, Hykes BL, Orchard RC, McCune BT, Kim KW, Nice TJ, Handley SA, Baldridge MT, Amarasinghe GK, Virgin HW. 2019. A secreted viral nonstructural protein determines intestinal norovirus pathogenesis. Cell Host Microbe 25:845–857.e5. https://doi.org/10.1016/j.chom.2019.04.005.
33. Borrego F. 2013. The CD300 molecules: an emerging family of regulators of the immune system. Blood 121:1951–1960. https://doi.org/10.1182/blood-2012-09-435057.
34. Lago N, Kaufmann FN, Negro-Demontel ML, Alí-Ruiz D, Ghisleni G, Rego N, Arcas-García A, Vitureira N, Jansen K, Souza LM, Silva RA, Lara DR, Pannunzio B, Abin-Carriquiry JA, Amo-Aparicio J, Martin-Otal C, Naya H, McGavern DB, Sayós J, López-Vales R, Kaster MP, Peluffo H. 2020. CD300f immunoreceptor is associated with major depressive disorder and decreased microglial metabolic fitness. Proc Natl Acad Sci U S A 117:6651–6662. https://doi.org/10.1073/pnas.1911816117.
35. Abadir E, Gasiorowski RE, Lai K, Kupresanin F, Romano A, Silveira PA, Lo TH, Fromm PD, Kennerson ML, Iland HJ, Ho PJ, Hogarth PM, Bradstock K, Hart DNJ, Clark GJ. 2019. CD300f epitopes are specific targets for acute myeloid leukemia with monocytic differentiation. Mol Oncol 13:2107–2120. https://doi.org/10.1002/1878-0261.12549.
36. Moshkovits I, Reichman H, Karo-Atar D, Rozenberg P, Zigmond E, Haberman Y, Ben Baruch-Morgenstern N, Lampinen M, Carlson M, Itan M, Denson LA, Varol C, Munitz A. 2017. A key requirement for CD300f in innate immune responses of eosinophils in colitis. Mucosal Immunol 10:172–183. https://doi.org/10.1038/mi.2016.37.
37. Martínez-Barriocanal Á, Arcas-García A, Magallon-Lorenz M, Ejarque-Ortíz A, Negro-Demontel ML, Comas-Casellas E, Schwartz S, Malhotra S, Montalban X, Peluffo H, Martín M, Comabella M, Sayós J. 2017. Effect of specific mutations in Cd300 complexes formation; potential implication of Cd300f in multiple sclerosis. Sci Rep 7:13544. https://doi.org/10.1038/s41598-017-12881-8.
38. Xi H, Katschke KJ, Helmy KY, Wark PA, Kljavin N, Clark H, Eastham-Anderson J, Shek T, Roose-Girma M, Ghilardi N, van Lookeren Campagne M. 2010. Negative regulation of autoimmune demyelination by the inhibitory receptor CLM-1. J Exp Med 207:7–16. https://doi.org/10.1084/jem.20091508.
39. von Moltke J, Ji M, Liang HE, Locksley RM. 2016. Tuft-cell-derived IL-25 regulates an intestinal ILC2-epithelial response circuit. Nature 529:221–225. https://doi.org/10.1038/nature16161.
40. Howitt MR, Lavoie S, Michaud M, Blum AM, Tran SV, Weinstock JV, Gallini CA, Redding K, Margolskee RF, Osborne LC, Artis D, Garrett WS. 2016. Tuft cells, taste-chemosensory cells, orchestrate parasite type 2 immunity in the gut. Science 351:1329–1333. https://doi.org/10.1126/science.aaf1648.
41. Gerbe F, Sidot E, Smyth DJ, Ohmoto M, Matsumoto I, Dardalhon V, Cesses P, Garnier L, Pouzolles M, Brulin B, Bruschi M, Harcus Y, Zimmermann VS, Taylor N, Maizels RM, Jay P. 2016. Intestinal epithelial tuft cells initiate type 2 mucosal immunity to helminth parasites. Nature 529:226–230. https://doi.org/10.1038/nature16527.
42. Grau KR, Zhu S, Peterson ST, Helm EW, Philip D, Phillips M, Hernandez A, Turula H, Frasse P, Graziano VR, Wilen CB, Wobus CE, Baldridge MT, Karst SM. 2020. The intestinal regionalization of acute norovirus infection is regulated by the microbiota via bile acid-mediated priming of type III interferon. Nat Microbiol 5:84–92. https://doi.org/10.1038/s41564-019-0602-7.
43. Wobus CE, Karst SM, Thackray LB, Chang KO, Sosnovtsev SV, Belliot G, Krug A, Mackenzie JM, Green KY, Virgin HW, IV. 2004. Replication of Norovirus in cell culture reveals a tropism for dendritic cells and macrophages. PLoS Biol 2:e432. https://doi.org/10.1371/journal.pbio.0020432.
44. Van Winkle JA, Robinson BA, Peters AM, Li L, Nouboussi RV, Mack M, Nice TJ. 2018. Persistence of systemic murine norovirus is maintained by inflammatory recruitment of susceptible myeloid cells. Cell Host Microbe 24:665–676.e4. https://doi.org/10.1016/j.chom.2018.10.003.
45. Mumphrey SM, Changotra H, Moore TN, Heimann-Nichols ER, Wobus CE, Reilly MJ, Moghadamfalahi M, Shukla D, Karst SM. 2007. Murine norovirus 1 infection is associated with histopathological changes in immunocompetent hosts, but clinical disease is prevented by STAT1-dependent interferon responses. J Virol 81:3251–3263. https://doi.org/10.1128/JVI.02096-06.
46. Westphalen CB, Asfaha S, Hayakawa Y, Takemoto Y, Lukin DJ, Nuber AH, Brandtner A, Setlik W, Remotti H, Muley A, Chen X, May R, Houchen CW, Fox JG, Gershon MD, Quante M, Wang TC. 2014. Long-lived intestinal tuft cells serve as colon cancer-initiating cells. J Clin Invest 124:1283–1295. https://doi.org/10.1172/JCI73434.
47. Grau KR, Roth AN, Zhu S, Hernandez A, Colliou N, DiVita BB, Philip DT, Riffe C, Giasson B, Wallet SM, Mohamadzadeh M, Karst SM. 2017. The major targets of acute norovirus infection are immune cells in the gut-associated lymphoid tissue. Nat Microbiol 2:1586–1591. https://doi.org/10.1038/s41564-017-0057-7.
48. Rickert RC, Roes J, Rajewsky K. 1997. B lymphocyte-specific, Cre-mediated mutagenesis in mice. Nucleic Acids Res 25:1317–1318. https://doi.org/10.1093/nar/25.6.1317.
49. Perry JW, Taube S, Wobus CE. 2009. Murine norovirus-1 entry into permissive macrophages and dendritic cells is pH-independent. Virus Res 143:125–129. https://doi.org/10.1016/j.virusres.2009.03.002.
50. Wu J, Wu H, An J, Ballantyne CM, Cyster JG. 2018. Critical role of integrin CD11c in splenic dendritic cell capture of missing-self CD47 cells to induce adaptive immunity. Proc Natl Acad Sci U S A 115:6786–6791. https://doi.org/10.1073/pnas.1805542115.
51. Clausen BE, Burkhardt C, Reith W, Renkawitz R, Förster I. 1999. Conditional gene targeting in macrophages and granulocytes using LysMcre mice. Transgenic Res 8:265–277. https://doi.org/10.1023/A:1008942828960.
52. Shi J, Hua L, Harmer D, Li P, Ren G. 2018. Cre driver mice targeting macrophages. Methods Mol Biol 1784:263–275. https://doi.org/10.1007/978-1-4939-7837-3_24.
53. Nakano T, Tahara-Hanaoka S, Nakahashi C, Can I, Totsuka N, Honda S, Shibuya K, Shibuya A. 2008. Activation of neutrophils by a novel triggering immunoglobulin-like receptor MAIR-IV. Mol Immunol 45:289–294. https://doi.org/10.1016/j.molimm.2007.04.011.

54. Can I, Tahara-Hanaoka S, Hitomi K, Nakano T, Nakahashi-Oda C, Kurita N, Honda S, Shibuya K, Shibuya A. 2008. Caspase-independent cell death by CD300LF (MAIR-V), an inhibitory immunoglobulin-like receptor on myeloid cells. J Immunol 180:207–213. https://doi.org/10.4049/jimmunol.180.1.207.
55. Matsukawa T, Izawa K, Isobe M, Takahashi M, Maehara A, Yamanishi Y, Kaitani A, Okumura K, Teshima T, Kitamura T, Kitaura J. 2016. Ceramide-CD300f binding suppresses experimental colitis by inhibiting ATP-mediated mast cell activation. Gut 65:777–787. https://doi.org/10.1136/gutjnl-2014-308900.
56. Takeshita S, Kaji K, Kudo A. 2000. Identification and characterization of the new osteoclast progenitor with macrophage phenotypes being able to differentiate into mature osteoclasts. J Bone Miner Res 15:1477–1488. https://doi.org/10.1359/jbmr.2000.15.8.1477.